



Title	Effect of Predamage on the Fracture Energy of Double-Network Hydrogels
Author(s)	Zheng, Yong; Wang, Yiru; Nakajima, Tasuku et al.
Citation	ACS macro letters, 13(2), 130-137 https://doi.org/10.1021/acsmacrolett.3c00702
Issue Date	2024-02-20
Doc URL	https://hdl.handle.net/2115/94098
Rights	This document is the Accepted Manuscript version of a Published Work that appeared in final form in ACS macro letters, copyright c American Chemical Society after peer review and technical editing by the publisher. To access the final edited and published work see https://pubs.acs.org/articlesonrequest/AOR-9HVR9WTGNNQYQQRWFXXKA
Type	journal article
File Information	Revised Manuscript.pdf



Effect of Pre-Damage on the Fracture Energy of Double-Network Hydrogels

Yong Zheng^{1}, Yiru Wang², Tasuku Nakajima^{1,3} and Jian Ping Gong^{1,3*}*

¹Institute for Chemical Reaction Design and Discovery (WPI-ICReDD), Hokkaido University, Sapporo 001-0021, Japan

²Graduate School of Life Science, Hokkaido University, Sapporo 001-0021, Japan

³Faculty of Advanced Life Science, Hokkaido University, Sapporo 001-0021, Japan

*Corresponding authors:

zhengyong@sci.hokudai.ac.jp (Yong Zheng)

gong@sci.hokudai.ac.jp (Jian Ping Gong).

ABSTRACT

Double-network (DN) hydrogels are tough soft materials and the high fracture resistance can be attributed to the formation of a large damage zone (internal fracture of the brittle first network) around the crack tip. In this work, we studied the effect of pre-damage in the brittle network on the fracture energy Γ_c of DN hydrogels. The pre-damage of the first network was induced by pre-stretching the DN gels to prestretch ratio λ_{pre} . Depending on the λ_{pre} in relative to the yielding stretch ratio λ_y , above which the brittle first network starts to break into discontinuous fragments inside DN gels, two

regimes were observed: Γ_c decreases monotonically with λ_{pre} in the regime of $\lambda_{pre} < \lambda_y$, mainly due to the decreasing contribution from the bulk internal damage; while Γ_c increases with λ_{pre} in the regime of $\lambda_{pre} > \lambda_y$. The latter can be understood by the release of hidden length of the stretchable network strands by the rupture of the brittle network, whereby the broken fragments of brittle network could serve as sliding crosslinks to further delocalize the stress concentration near the crack tip and prevent chain scissions.

The well accepted Griffith's energetic criterion predicts the crack initiation based on the competition between two quantities: the strain energy release rate G that provides the driving force for crack propagation, and the fracture energy Γ to resist crack propagation.¹⁻⁴ To propagate a crack, the former needs to reach or exceed the latter. The models established based on this energy consideration have so far been instrumental in predicting the fracture of covalent polymer network materials that are both elastic and viscoelastic.¹⁻¹⁰

In recent decades, soft materials have found numerous emerging applications in fields including bioengineering materials, drug delivery, wearable electronics, and soft robotics.¹¹⁻²⁴ A variety of efforts in the field of soft materials have been devoted to designing materials as robust as possible to resist initial crack initiation, taking advantages of fracture toughness at crack initiation as the most important design consideration. Among some great efforts, the double-network (DN) concept stands out as an extraordinary strategy for toughening soft materials including gels, elastomers as

well as composite materials.²⁵⁻³² The DN gels are a typical and classical example of strong and tough gels, which were originally invented by Gong's group in 2003.³³ The DN gels are characterized by a special network structure consisting of two types of interpenetrating polymer components with contrasting physical natures; *i.e.*, a stiff and brittle first network with dilute, densely crosslinked short chains, which serves as sacrificial bonds, and a soft and ductile second network with concentrated, loosely cross-linked long chains, which acts as stretchable matrix. Immense efforts have been taken to clarify the origin of its extraordinary fracture toughness, which emphasized the importance of the brittle network as sacrificial bonds inside DN gels.³⁴⁻⁴⁵ Upon deformation, the brittle network suffers significant damage with an abundance of covalent bond scissions dissipating large amounts of energy, while the stretchable network can keep the integrity of the material without failure. This internal damage also occurs ahead of the crack tip accompanied by the formation of a damage zone around the crack tip dissipating a huge amount of energy, which contributes to the extraordinarily high fracture energy of DN gels. In a recent report, by virtue of mechanochemical techniques, Gong's group has succeeded in visualizing the damage and quantifying stress, strain, as well as the fracture energy contribution around the crack tip of DN gels.⁴² By comparing the fracture energy of DN gels to its counterpart with damage, it is suggested that in addition to energy dissipation in a yield region (so-called damage zone in the previous study) ahead of the crack tip, the dissipation in the wide pre-yielding region and the intrinsic fracture energy also have a large contribution to the fracture energy. Despite that some of the previous studies have measured the

fracture energy of DN gels with damage^{42, 46}, a systematic control of pre-damage and a careful examination on the effect of pre-damage on the fracture energy of DN gels at crack initiation is still lacking.

In this study, we systematically control the extent of pre-damage in DN gels and reveal its effect on the crack initiation for the DN hydrogels by a fracture energy analysis on the pure-shear crack tests and single-edge notch tests. Our experiments were conducted with DN hydrogels consisting of poly(2-acrylamido-2-methylpropane sulfonic acid sodium salt) (PNaAMPS) as the brittle first network and polyacrylamide (PAAm) as the soft second network, both of which were synthesized via a two-step polymerization process following the literature.⁴¹ The synthesized DN gel demonstrates typical mechanical behaviors and extremely high stretchability as reported in previous studies,^{34, 43} exhibiting obvious stress-yielding behavior at relatively small deformation and significant strain-hardening behavior at large deformation (Figure S1). Owing to the combination of two elastic covalently crosslinked interpenetrated networks, DN hydrogels are a relatively simple system in which no rate-dependent deformation or damage behaviors are involved, and accumulative damage can be induced in a controllable manner prior to crack tests.^{44, 47, 48}

In this paper, we are specifically interested in how the accumulative damage would affect the fracture energy of DN gels. For this, prior to crack tests, we first induce different level of internal damage in the brittle first network of DN gels by applying various extents of stretch (i.e., λ_{pre}) to the unnotched DN gels (Figure 1A). During this pre-stretch process, strands of the brittle first network reaching their stretching limits

break progressively, resulting in a non-recoverable hysteresis loop in its loading-unloading stress curves (Figure 1B(i) and S2). The extent of internal damage quantified by the hysteresis loop area $U_{\text{hys}}(\lambda_{\text{pre}})$ considerably increases with the increase of λ_{pre} above 1.5, indicating the progressively enhanced internal damage with the increase of prestretch (Figure S2C). Accordingly, we obtain DN gels with various extents of internal damage by varying λ_{pre} . We denote DN gels with pre-damage as DN- λ_{pre} , and DN-1.0 corresponds to the virgin DN gel. For the pre-damaged DN- λ_{pre} gel, when subjected to loading-unloading cycle, its mechanical behavior highly depends on the relation between the posed stretch ratio λ_{max} and the pre-stretch ratio λ_{pre} (Figure 1B). When $\lambda_{\text{max}} < \lambda_{\text{pre}}$, the loading and unloading curves overlap because no internal damage occurs (Figure 1B(ii)), and the area under the loading curve corresponds to the stored strain energy under loading (Figure 1B(ii), pink colored area); when $\lambda_{\text{max}} > \lambda_{\text{pre}}$, internal damage occurs in the loading region of λ between λ_{pre} and λ_{max} , resulting in hysteresis between the loading and unloading curves (Figure 1B(iii), green colored area). The material parameters including the loading energy density W_{load} , the stored strain energy density W_{el} ($=W_{\text{unload}}$), and the dissipated energy density U_{diss} ($=U_{\text{hys}}$) for the pre-damaged DN- λ_{pre} gels are summarized in Figure S3A–C.

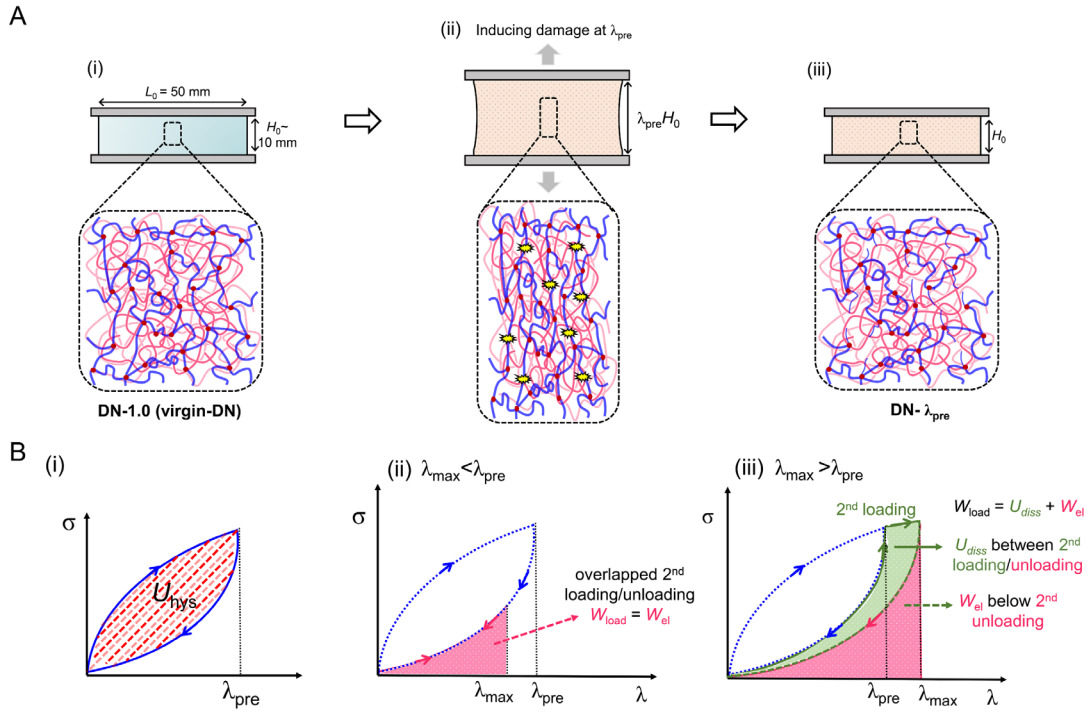


Figure 1. Inducing internal damage to DN gels. (A) Schematic illustration of experiments to induce internal damage to DN gels by stretching and the corresponding structure change of the brittle first network (blue). The DN gels after inducing damage are denoted as DN- λ_{pre} . (B) The DN- λ_{pre} samples subjected to the experiment as described in (A) showed a hysteresis loop in the loading-unloading curves, indicating pre-induced internal damage of the brittle first network (i). The typical loading-unloading behaviors for pre-damaged DN- λ_{pre} gels subjected to a second loading at $\lambda_{max} < \lambda_{pre}$ (ii) and $\lambda_{max} > \lambda_{pre}$ (iii).

To examine how accumulative damage affects the crack initiation in these pre-damaged DN gels, we use a razor blade to introduce a large notch into the edge of the DN- λ_{pre} gels and then load the notched sample to see how the critical stretch ratio λ_c at the onset of crack propagation changes. To observe the crack growth during loading process, we adopt the experimental setup to perform real-time imaging of birefringence (Figure 2A and S4).^{43, 49} Such an experimental setup can not only capture the crack growth behavior but also reveal the degree of network strand orientation ahead of crack tip during deformation. In an early report, we applied this experimental setup to quantify the damage zone area ahead of crack tip, where the second network strands are in highly stretched state along the tensile direction to show strong birefringence, for DN gels.⁴³

The stress curves of the pre-damaged DN- λ_{pre} gels during crack test are shown in Figure 2B. As elucidated in the previous study, the yielding stretch ratio λ_y (~ 3.20) of DN gels observed from uniaxial tensile curve (Figure S1) corresponds to the point above which the brittle first network is broken into discontinuous structure along the sample width direction.⁵⁰ Accordingly, we divide the dependence of the stress curves on the λ_{pre} into two regimes based on the relation between λ_{pre} and λ_y : regime I ($\lambda_{\text{pre}} < \lambda_y$) in which the brittle first network still has continuous structure and mainly carries the load and regime II ($\lambda_{\text{pre}} > \lambda_y$) in which the brittle first network has been damaged into discontinuous fragments and the stretchable second network becomes mainly carrying the load. **Figure 2C** shows the dependence of the critical stretch ratio λ_c at the

onset of crack propagation on the λ_{pre} . In regime I, $\lambda_c > \lambda_{pre}$ and λ_c is nearly a constant around 2.6 for $\lambda_{pre} \leq 2.0$ but slightly increases with λ_{pre} for $\lambda_{pre} = 2.0-3.0$; while in regime II, λ_c is nearly identical to λ_{pre} .

Here we estimate the fracture energy of these pre-damaged DN- λ_{pre} gels. The work of loading an unnotched sample to a maximum stretch ratio (λ_{max}), denoted as $W_{load}(\lambda_{max})$, decreases with the increase of λ_{pre} (Figure S3A). The apparent fracture energy Γ_c at crack initiation for DN- λ_{pre} is a function λ_{pre} and can be determined by $\Gamma_c = G_c = W_{load}(\lambda_c)H_0$.^{3, 5} For DN- λ_{pre} gels in regime I ($\lambda_{pre} < \lambda_y$), Γ_c decreases monotonically from 4220 to 2230 J/m² because of the decrease of $U_{hys}(\lambda_c)$; while for DN- λ_{pre} gels in regime II ($\lambda_{pre} > \lambda_y$), it is interesting to see that Γ_c slightly increases from 2000 to 2600 J/m² (Figure 3A).

Since the DN gels dissipate energy during loading due to internal fracture, the applied loading energy is partially used for breaking the first network in the bulk, not all dissipated near the vicinity of the crack. Here, we seek to separate the apparent fracture energy Γ_c of DN gels into two contributions: (1) Γ_{bulk} that is consumed by the sacrificial damage of brittle network in the bulk (far from a crack) and (2) Γ_{tip} that is consumed in the process zone near the vicinity of crack tip (Figure 3C). We estimated Γ_{bulk} from the mechanical hysteresis area U_{diss} (Figure S3C) as $\Gamma_{bulk} = U_{diss}H_0$. For a pre-damaged DN- λ_{pre} gel, the dissipated energy density U_{diss} to a critical stretch ratio of λ_c could be estimated from the total dissipated energy density $U_{hys}(\lambda_c)$ of the virgin sample, taking away the part used for damage during pre-stretch, $U_{hys}(\lambda_{pre})$. Namely, $U_{diss}(\lambda_c) = U_{hys}(\lambda_c) - U_{hys}(\lambda_{pre})$. Here, we apply the Griffith law by

correlating the stored strain energy per unit area G_{el} with the energy dissipation at the crack tip, $\Gamma_{tip} = G_{el} = W_{el}(\lambda_c)H_0$, where $W_{el}(\lambda_c)$ is the stored elastic energy density of the unnotched sample stretched to λ_c (Figure S3B). As summarized in Figure 3B, Γ_{bulk} decreases remarkably with the increase of λ_{pre} from 2870 to 420 J/m² in regime I ($\lambda_{pre} \leq 3.0 < \lambda_y$) and becomes zero in regime II ($\lambda_{pre} \geq 3.25 > \lambda_y$), which accounts for the initially decreasing trend of Γ_c . It is interesting to note that Γ_{tip} exhibits slightly increasing tendency from 1350 to 1800 J/m² in regime I ($\lambda_{pre} \leq 3.0 < \lambda_y$), then moderately increases to 2500 J/m² in regime II ($\lambda_{pre} \geq 3.25 > \lambda_y$). These results show that the local fracture energy at crack vicinity has a quite large value and slightly increases with pre-damage of the first network.

As the local fracture energy Γ_{tip} at crack initiation can be considered as the sum of the energy dissipation for local yielding zone formation Γ_{yield} and that for breaking the strands across the crack plane Γ_0 (Figure 3C),⁴⁴ $\Gamma_{tip} = \Gamma_{yield} + \Gamma_0$. To clarify the increasing tendency of Γ_{tip} , we next discuss the trend of Γ_{yield} and Γ_0 with λ_{pre} . $\Gamma_{yield} \approx U_{dis,y}h_y$, here $U_{dis,y}$ is the energy dissipation density inside the yielding zone and h_y is the yielding zone size in the undeformed state. $U_{dis,y}$ decreases with λ_{pre} owing to the increased pre-damage in the bulk. The area to exhibit strong birefringence at the crack tip slightly decreases as the λ_{pre} increases (Figure 4A, B). The birefringence area S_c at deformed state also exhibits slightly decreasing trend with the increase of λ_{pre} at $\lambda_{pre} \leq 3.0$ (regime I) and then reaches a plateau value at $\lambda_{pre} \geq 3.25$ (regime II) (Figure 4C). Since $h_y \sim S_c^{0.5}$,⁴³ the yielding zone size shows the decreasing tendency as λ_{pre} increases. Given the common decreasing trend of both $U_{dis,y}$ and

h_y , the energy dissipation consumed for local yielding zone formation Γ_{yield} decreases with λ_{pre} . Thus, it comes to a surprising conclusion that the Γ_0 must exhibit a significant increasing trend to prevail over the decreasing trend of Γ_{yield} , ensuring that Γ_{tip} is increasing with the increase of λ_{pre} (Figure 3B). This energy consideration implies a surprising finding that the intrinsic fracture energy Γ_0 to break stretchable strand layers crossing the crack plane is not an invariable constant as we previously assumed and as measured for the as-prepared SN PAAm hydrogel (670 J/m², Figure S5). It surprisingly gets enhanced with the pre-damage in brittle first network. This enhancement effect of Γ_0 by pre-damage has similarity to a recent report showing that preferential bond scission of the weak bonds releases extra hidden length, which share the load along the primary chains ahead of crack front, providing a substantive toughening effect.⁵¹ One possible effect is from softening of the DN gel at large λ_{pre} . The softening effect by pre-induced damage can make the stretchable strands more bearable for a large deformation ahead of crack tip, which possibly accounts for the enhanced Γ_0 . Another plausible effect is that the broken fragments of brittle network could serve as sliding crosslinks to further delocalize the stress concentration near the crack tip and prevent chain scissions, like that discovered in highly entangled network systems.^{52,53}

It can be deduced from the increasing tendency of Γ_{tip} (Figure 3B) that if an extremely large extent of pre-damage can be imposed to DN gels by inducing λ_{pre} close to its maximum stretchability, the increasing contribution of Γ_{tip} near the vicinity of crack tip may prevail the decreasing contribution of Γ_{bulk} , making the pre-

damaged DN gels even tougher than the undamaged virgin DN gels.

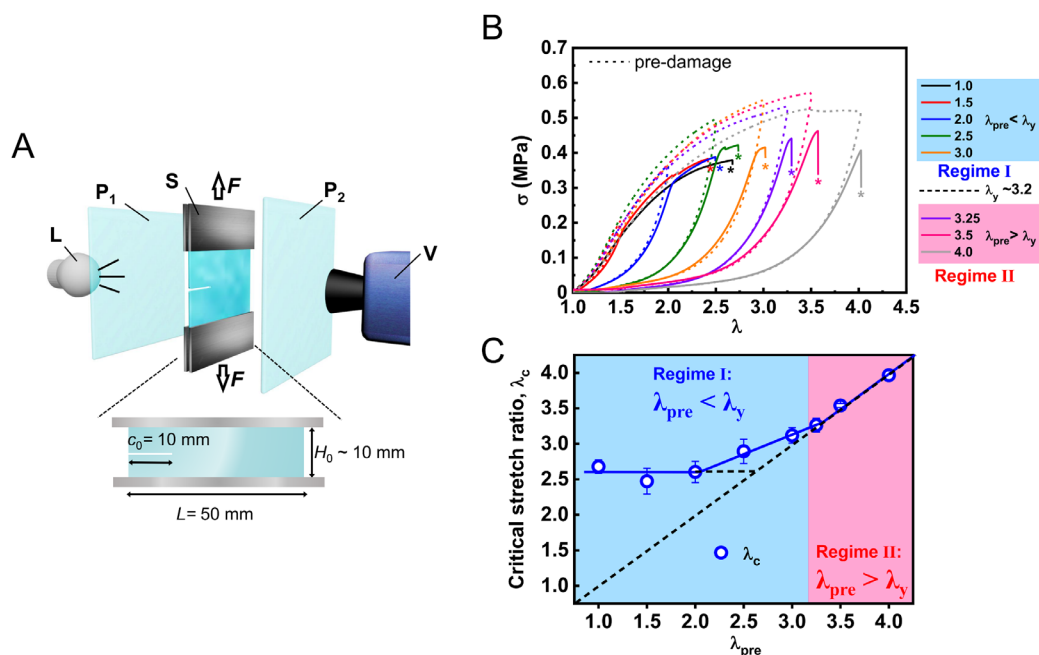


Figure 2. Effect of pre-stretching ratio λ_{pre} on the crack initiation of pre-damaged DN hydrogels. (A) Schematic for observation of the real-time birefringence of the fracture process for pre-damaged DN gels in a pure shear test. Abbreviations: L, lamp; P₁ and P₂, crossed circular polarized films; S, sample; V, video camera. Reproduced from ref (43). Copyright 2021 National Academy of Sciences. (B) The stress-stretch ratio curves for DN- λ_{pre} gels in pure-shear fracture tests. The dotted lines show loading-unloading cycles of unnotched samples to induce pre-damage prior to fracture test. The loading velocity $v = 50$ mm/min. (C) Dependence of critical stretch ratio λ_c at the onset of crack propagation on λ_{pre} .

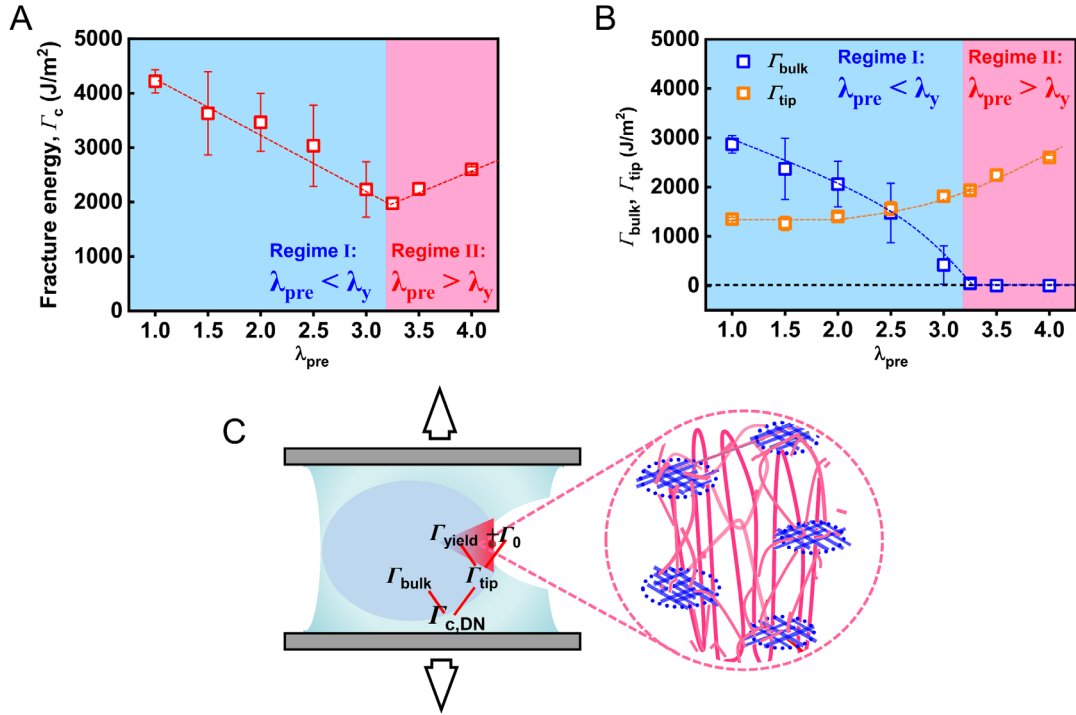


Figure 3. Fracture energy of pre-damaged DN hydrogels at crack initiation. (A) Apparent fracture energy $\Gamma_c = G_c = W_{load}(\lambda_c)H_0$. (B) Fracture energy for bulk internal damage $\Gamma_{bulk} = U_{dis}(\lambda_c)H_0$ and consumed in the vicinity of crack tip $\Gamma_{tip} = G_{el} = W_{el}(\lambda_c)H_0$, where $\Gamma_c = \Gamma_{bulk} + \Gamma_{tip}$. $W_{load}(\lambda_c)$, $W_{el}(\lambda_c)$ and $U_{dis}(\lambda_c)$ for various λ_{pre} are obtained from **Figure S3**. The average is collected from 3 measurements for each DN gel. (C) Schematic illustration on the various energy contributions to the apparent fracture energy of DN gels.

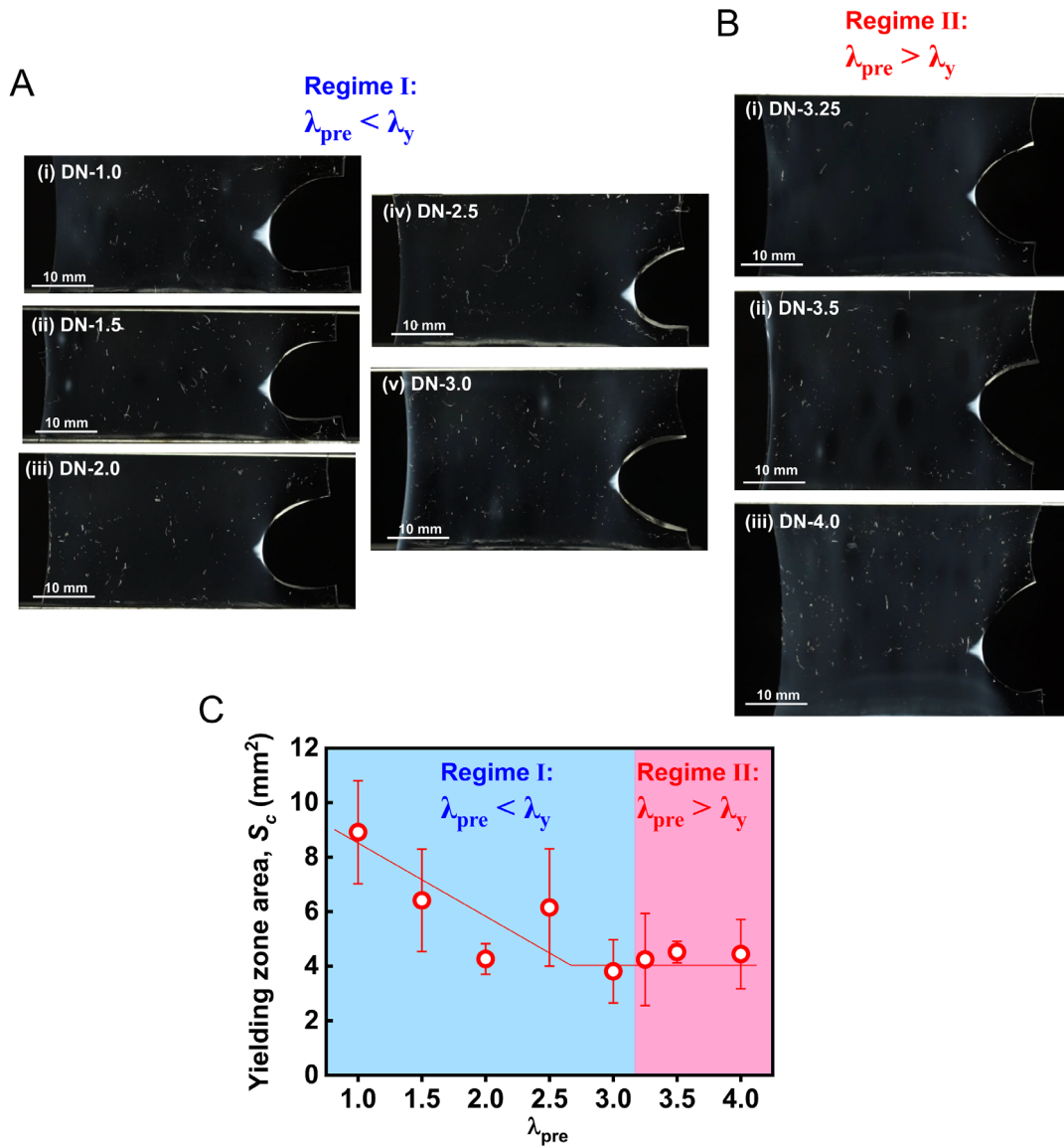


Figure 4. Yielding zone area of pre-damaged DN hydrogels at crack initiation. (A, B) Birefringence image of various DN- λ_{pre} sample observed by the birefringence experimental setup: (A) regime I ($\lambda_{pre} < \lambda_y$) and (B) regime II ($\lambda_{pre} > \lambda_y$). Strong birefringence area around the crack tip indicates yielding zone in which the 2nd network strands are strongly oriented. (C) Pre-stretch ratio λ_{pre} dependence of yielding zone area S_c determined from (A, B).

The extent of pre-damage is restricted by the maximum stretchability of DN hydrogels under a pure shear configuration with a large width ($L_0 = 50$ mm) owing to the strong stress concentration at the clamped positions. To induce extremely large pre-damage in DN gels, we use a strip configuration with a much smaller width ($L_0 = 10$

mm) (Figure 5A). The λ_{pre} can be applied as large as 16.0, much larger than that can be imposed in pure shear configuration ($\lambda_{\text{pre}} \leq 4.0$). To substantiate the enhanced toughening effect with the pre-induced damage in brittle first network, we perform single-edge crack tests on the DN- λ_{pre} gels with systematically varied initial crack length c_0 . We select three specific λ_{pre} : (1) $\lambda_{\text{pre}} = 1.0$ corresponds to the virgin DN gels without pre-damage, (2) $\lambda_{\text{pre}} = 2.4$ corresponds to the DN gels with a small amount of pre-damage (prior to yielding) and (3) $\lambda_{\text{pre}} = 16.0$ corresponds to the severely pre-damaged DN gels in which the brittle first network is completely broken to small fragments serving as sliding cross-links. It should be noted that for the strip configuration, the yielding stretch ratio of the DN gel is determined as ~ 2.7 . The corresponding stress curves of DN-1.0, DN-2.4 and DN-16.0 subjected to single-edge crack tests with varied c_0 are shown in Figure S6–S8.

Similar to that in the pure-shear tests, the critical strain energy density $W_b(\lambda_c)$ in the single-edge tests can also be obtained by $W_b(\lambda_c) = \int_1^{\lambda_c} \sigma_{\text{un-notched}} d\lambda$, where λ_c is the critical stretch ratio at the onset of crack growth for the notched sample. We find that in the large c_0 range of 0.5-8.0 mm, the $W_b(\lambda_c)$ for these three series of DN- λ_{pre} gels all roughly follows a general relation of $W_b(\lambda_c) \propto c_0^{-1}$ (Figure 5B). Note that the deviations in the small c_0 range from such a general relation of $W_b(\lambda_c) \propto c_0^{-1}$ for the DN-1.0 and DN-2.4 gels suggest a critical flaw-sensitivity related length scale c^* , below which the DN gel can exhibit necking expansion behaviors before crack propagation showing its flaw-insensitivity (Figure S6B(i) and S7B(i)). This general relation of $W_b(\lambda_c) \propto c_0^{-1}$ has also been found in a previous study by Suo's group

researching on the single-edge tests of DN hydrogels,⁵³ despite a different composition of DN hydrogels and a different sample shape, suggesting that this relation is somehow general for DN hydrogels. It is inferred from their study that the product of $W_b(\lambda_c)c_0$ may qualitatively represent the material-specific toughness simply using the prediction of linear elasticity to compare with the experiment.⁵⁴ Here, we compare the material-specific toughness between different DN- λ_{pre} gels by simply comparing the product of $W_b(\lambda_c)c_0$. The data series for the severely pre-damaged DN-16.0 nicely fall into a line well above that for the DN-1.0 without damage, and the data series for the slightly pre-damaged DN-2.4 is below that for DN-16.0 and DN-1.0 (Figure 5B). The severely pre-damaged DN-16.0 possibly have the highest fracture toughness ($W_b(\lambda_c)c_0=655 \text{ J/m}^2$), followed by the DN-1.0 ($W_b(\lambda_c)c_0 =408 \text{ J/m}^2$), and the slightly pre-damaged DN-2.4 ($W_b(\lambda_c)c_0=264 \text{ J/m}^2$) has the lowest fracture toughness among these three DN hydrogels. The decreased fracture toughness for the slightly pre-damaged DN-2.4 compared with the DN-1.0 is in good consistence with the decreasing Γ_c measured by pure-shear tests (the regime I in Figure 3A). More importantly, the enhanced fracture toughness for the severely pre-damaged DN-16.0 in comparison to DN-1.0 strongly supports a substantive toughening effect by the preferential bond scission of the brittle network. After severe pre-damage, the originally brittle network with continuous structure was broken into discontinuous fragments; during such process, it releases extra hidden length in the stretchable strands and further share the load along the primary chains ahead of crack front to delocalize the stress concentration near the crack tip and prevent chain scissions. In addition, the much more enhanced stress curves and

the corresponding $W_b(\lambda_c)$ for the pre-damaged DN-16.0 gels in comparison to these of the as prepared PAAM gels (at $c_0 = 0$ and 2 mm) (Figure 5B and S8), suggest that the broken fragments of brittle network serve as sliding crosslinks to further strengthen and toughen DN gels.^{55,56}

In summary, we have carefully revealed the effect of pre-damage on the crack initiation for the DN hydrogels by a systematic analysis on the pure-shear and single-edge notch tests. It is clear that the fracture energy of DN hydrogels at crack initiation strongly depends on the extent of pre-damage in the brittle network strands, namely, the pre-stretch ratio λ_{pre} . In the regime I ($\lambda_{pre} < \lambda_y$), in which the pre-damage is insufficient to cause the brittle first network broken catastrophically with discontinuous fragment structure inside DN gels, Γ_c decreases monotonically mainly due to the decreasing contribution of Γ_{bulk} from the bulk internal damage; while in regime II ($\lambda_{pre} > \lambda_y$), in which the brittle first network start to be damaged into discontinuous fragments, Γ_c begins to increase due to the increased local fracture energy Γ_{tip} at crack vicinity. This surprising increment in the fracture toughness possibly originates from a toughening effect by the released hidden length of the stretchable strands by the rupture of the brittle network, whereby the broken fragments of brittle network could serve as sliding crosslinks to further delocalize the stress concentration near the crack tip and prevent chain scissions.

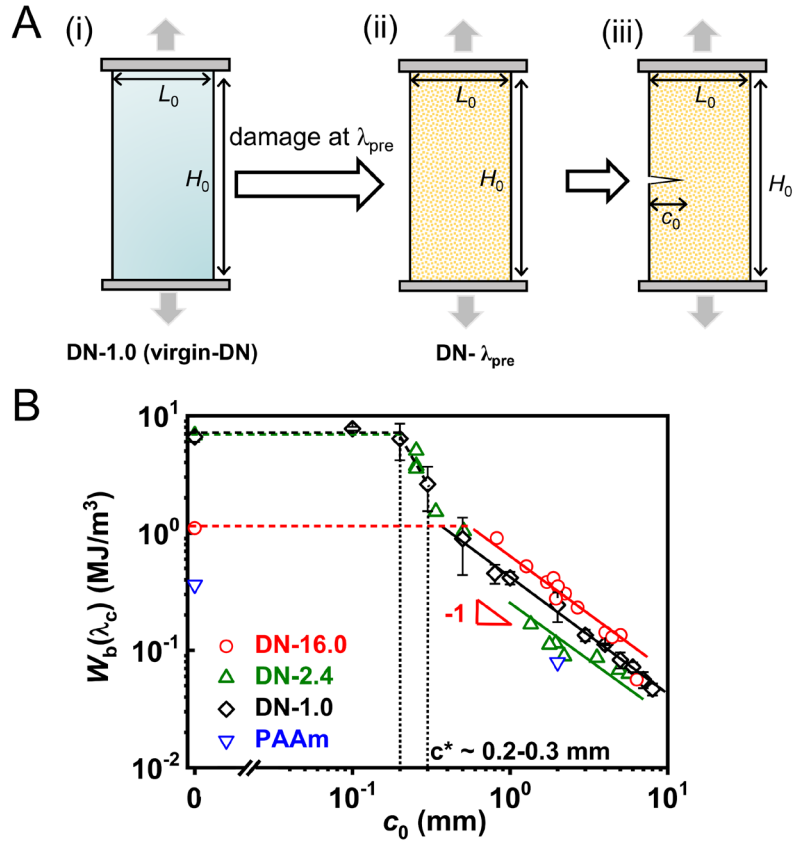


Figure 5. Single-edge notch crack tests on the severely pre-damaged DN gels. (A) Schematic illustration of experiments to induce internal damage to DN gels by stretching under a single-edge notch configuration prior to the single-edge notch tests. Sample configuration: sample width $L_0 = 10$ mm, sample height $H_0 = 35$ mm and varied crack length c_0 . The DN gels after inducing damage are denoted as DN- λ_{pre} . (B) The critical strain energy density $W_b(\lambda_c)$ as a function of initial crack length c_0 for DN- λ_{pre} with different λ_{pre} . The critical length scale c^* related to the flaw-sensitivity of DN-1.0 gels is around 0.2-0.3 mm. The data for PAAm SN hydrogels with crack length $c_0 = 2$ mm and without notch are also included for comparison.

ASSOCIATED CONTENT

Supporting Information.

Figure S1. Uniaxial tensile stress-stretch ratio curve of DN gel used in this work.

Figure S2. Cyclic tensile test with increased stretch ratio performed in virgin DN gels.

Figure S3. The material parameters of the pre-damaged DN- λ_{pre} gels.

Figure S4. Illustration of the real-time birefringence observation.

Figure S5. Pure shear fracture curves for the PAAm single-network (SN) hydrogels.

Figure S6. Single-edge notch fracture curves for the DN-1.0 hydrogels.

Figure S7. Single-edge notch fracture curves for the DN-2.4 hydrogels.

Figure S8. Single-edge notch fracture curves for the DN-16.0 hydrogels and PAAm hydrogels.

Supplementary text on the materials and methods related with the hydrogel synthesis, the uniaxial tensile tests, the method to induce internal damage to DN gels prior to pure-shear crack tests, the cyclic tensile test in pure-shear geometry and the calculation of U_{hys} and W_{el} , the pure-shear fracture tests and the real-time birefringence observation, and the single-edge notch tests.

AUTHOR INFORMATION

Corresponding Authors

*E-mail address: zhengyong@sci.hokudai.ac.jp (Yong Zheng).

*E-mail address: gong@sci.hokudai.ac.jp (Jian Ping Gong).

Author Contributions

The manuscript was written through contributions of all authors. All authors have given approval to the final version of the manuscript.

Notes

The authors declare no competing financial interest.

ACKNOWLEDGMENT

This research is supported by the Japan Society for the Promotion of Science (JSPS) KAKENHI (grant nos. JP22H04968, JP22K21342) and by JST, PRESTO grant Number JPMJPR2098.

REFERENCES

- (1) Griffith, A. A. VI. The phenomena of rupture and flow in solids. *Philosophical transactions of the royal society of london. Series A, containing papers of a mathematical or physical character* **1921**, 221, 163–198.
- (2) Shen, T.; Song, Z.; Cai, S.; Vernerey, F. J. Nonsteady fracture of transient networks: The case of vitrimer. *Proc. Natl. Acad. Sci. U.S.A.* **2021**, 118, e2105974118.
- (3) Long, R.; Hui, C.-Y. Fracture toughness of hydrogels: measurement and interpretation. *Soft Matter* **2016**, 12, 8069–8086.
- (4) Creton, C.; Ciccotti, M. Fracture and adhesion of soft materials: a review. *Rep. Prog. Phys.* **2016**, 79, 046601.
- (5) Rivlin, R.; Thomas, A. G. Rupture of rubber. I. Characteristic energy for tearing. *J. Polym. Sci.* **1953**, 10, 291–318.
- (6) Wang, X.; Hong, W. Delayed fracture in gels. *Soft Matter* **2012**, 8, 8171–8178.
- (7) Glassmaker, N.; Hui, C.; Yamaguchi, T.; Creton, C. Detachment of stretched viscoelastic fibrils. *Eur. Phys. J. E* **2008**, 25, 253–266.
- (8) Schapery, R. A. A theory of crack initiation and growth in viscoelastic media: I. Theoretical development. *Int. J. Fract.* **1975**, 11, 141–159.
- (9) Schapery, R. A. Correspondence principles and a generalized J integral for large deformation and fracture analysis of viscoelastic media. *Int. J. Fract.* **1984**, 25, 195–223.
- (10) Nguyen, T.; Govindjee, S. Numerical study of geometric constraint and cohesive parameters in steady-state viscoelastic crack growth. *Int. J. Fract.* **2006**, 141, 255–268.

- (11) Kim, D.-H.; Lu, N.; Ma, R.; Kim, Y.-S.; Kim, R.-H.; Wang, S.; Wu, J.; Won, S. M.; Tao, H.; Islam, A. Epidermal electronics. *Science* **2011**, 333, 838–843.
- (12) Takei, K.; Takahashi, T.; Ho, J. C.; Ko, H.; Gillies, A. G.; Leu, P. W.; Fearing, R. S.; Javey, A. Nanowire active-matrix circuitry for low-voltage macroscale artificial skin. *Nat. Mater.* **2010**, 9, 821–826.
- (13) Hoffman, A. S. Hydrogels for biomedical applications. *Adv. Drug Deliv. Rev.* **2012**, 64, 18–23.
- (14) Haque, M. A.; Kurokawa, T.; Gong, J. P. Super tough double network hydrogels and their application as biomaterials. *Polymer* **2012**, 53, 1805–1822.
- (15) Yuk, H.; Lin, S.; Ma, C.; Takaffoli, M.; Fang, N. X.; Zhao, X. Hydraulic hydrogel actuators and robots optically and sonically camouflaged in water. *Nat. Commun.* **2017**, 8, 1–12.
- (16) Yang, C.; Suo, Z. Hydrogel ionotronics. *Nat. Rev. Mater.* **2018**, 3, 125–142.
- (17) Zhao, X.; Chen, X.; Yuk, H.; Lin, S.; Liu, X.; Parada, G. Soft materials by design: unconventional polymer networks give extreme properties. *Chem. Rev.* **2021**, 121, 4309–4372.
- (18) Keplinger, C.; Sun, J.-Y.; Foo, C. C.; Rothemund, P.; Whitesides, G. M.; Suo, Z. Stretchable, transparent, ionic conductors. *Science* **2013**, 341, 984–987.
- (19) Lin, S.; Yuk, H.; Zhang, T.; Parada, G. A.; Koo, H.; Yu, C.; Zhao, X. Stretchable hydrogel electronics and devices. *Adv. Mater.* **2016**, 28, 4497–4505.
- (20) Rogers, J. A.; Someya, T.; Huang, Y. Materials and mechanics for stretchable electronics. *Science* **2010**, 327, 1603–1607.
- (21) Rogers, J.; Bao, Z.; Lee, T.-W. Wearable bioelectronics: opportunities for chemistry. *Acc. Chem. Res.* **2019**, 52, 521–522.
- (22) Kang, J.; Tok, J. B.-H.; Bao, Z. Self-healing soft electronics. *Nat. Electron.* **2019**, 2, 144–150.
- (23) Li, G.; Chen, X.; Zhou, F.; Liang, Y.; Xiao, Y.; Cao, X.; Zhang, Z.; Zhang, M.; Wu, B.; Yin, S. Self-powered soft robot in the Mariana Trench. *Nature* **2021**, 591, 66–71.

- (24) Zhao, Y.; Chi, Y.; Hong, Y.; Li, Y.; Yang, S.; Yin, J. Twisting for soft intelligent autonomous robot in unstructured environments. *Proc. Natl. Acad. Sci. U.S.A.* **2022**, 119 (22), e2200265119.
- (25) Ducrot, E.; Chen, Y.; Bulters, M.; Sijbesma, R. P.; Creton, C. Toughening elastomers with sacrificial bonds and watching them break. *Science* **2014**, 344, 186–189.
- (26) Ducrot, E.; Creton, C. Characterizing large strain elasticity of brittle elastomeric networks by embedding them in a soft extensible matrix. *Adv. Funct. Mater.* **2016**, 26, 2482–2492.
- (27) Millereau, P.; Ducrot, E.; Clough, J. M.; Wiseman, M. E.; Brown, H. R.; Sijbesma, R. P.; Creton, C. Mechanics of elastomeric molecular composites. *Proc. Natl. Acad. Sci. U.S.A.* **2018**, 115, 9110–9115.
- (28) Zheng, Y.; Kiyama, R.; Matsuda, T.; Cui, K.; Li, X.; Cui, W.; Guo, Y.; Nakajima, T.; Kurokawa, T.; Gong, J. P. Nanophase Separation in Immiscible Double Network Elastomers Induces Synergetic Strengthening, Toughening, and Fatigue Resistance. *Chem. Mater.* **2021**, 33, 3321–3334.
- (29) Matsuda, T.; Nakajima, T.; Gong, J. P. Fabrication of tough and stretchable hybrid double-network elastomers using ionic dissociation of polyelectrolyte in nonaqueous media. *Chem. Mater.* **2019**, 31, 3766–3776.
- (30) Zhang, X.; Tang, Z.; Huang, J.; Lin, T.; Guo, B. Strikingly improved toughness of nonpolar rubber by incorporating sacrificial network at small fraction. *J. Polym. Sci. B: Polym. Phys.* **2016**, 54, 781–786.
- (31) King, D. R.; Okumura, T.; Takahashi, R.; Kurokawa, T.; Gong, J. P. Macroscale double networks: design criteria for optimizing strength and toughness. *ACS Appl. Mater. Interfaces.* **2019**, 11, 35343–35353.
- (32) Cui, W.; Huang, Y.; Chen, L.; Zheng, Y.; Saruwatari, Y.; Hui, C.-Y.; Kurokawa, T.; King, D. R.; Gong, J. P. Tiny yet tough: Maximizing the toughness of fiber-reinforced soft composites in the absence of a fiber-fracture mechanism. *Matter* **2021**, 4, 3646–3661.

- (33) Gong, J. P.; Katsuyama, Y.; Kurokawa, T.; Osada, Y. Double-network hydrogels with extremely high mechanical strength. *Adv. Mater.* **2003**, *15*, 1155–1158.
- (34) Gong, J. P. Why are double network hydrogels so tough? *Soft Matter* **2010**, *6*, 2583–2590.
- (35) Tanaka, Y.; Kuwabara, R.; Na, Y.-H.; Kurokawa, T.; Gong, J. P.; Osada, Y. Determination of fracture energy of high strength double network hydrogels. *J. Phys. Chem. B.* **2005**, *109*, 11559–11562.
- (36) Na, Y.-H.; Tanaka, Y.; Kawauchi, Y.; Furukawa, H.; Sumiyoshi, T.; Gong, J. P.; Osada, Y. Necking phenomenon of double-network gels. *Macromolecules* **2006**, *39*, 4641–4645.
- (37) Tanaka, Y. A local damage model for anomalous high toughness of double-network gels. *EPL (Europhysics Letters)* **2007**, *78*, 56005.
- (38) Webber, R. E.; Creton, C.; Brown, H. R.; Gong, J. P. Large strain hysteresis and Mullins effect of tough double-network hydrogels. *Macromolecules* **2007**, *40*, 2919–2927.
- (39) Brown, H. R. A model of the fracture of double network gels. *Macromolecules* **2007**, *40*, 3815–3818.
- (40) Yu, Q. M.; Tanaka, Y.; Furukawa, H.; Kurokawa, T.; Gong, J. P. Direct observation of damage zone around crack tips in double-network gels. *Macromolecules* **2009**, *42*, 3852–3855.
- (41) Ahmed, S.; Nakajima, T.; Kurokawa, T.; Haque, M. A.; Gong, J. P. Brittle–ductile transition of double network hydrogels: Mechanical balance of two networks as the key factor. *Polymer* **2014**, *55*, 914–923.
- (42) Matsuda, T.; Kawakami, R.; Nakajima, T.; Hane, Y.; Gong, J. P. Revisiting the Origins of the Fracture Energy of Tough Double-Network Hydrogels with Quantitative Mechanochemical Characterization of the Damage Zone. *Macromolecules* **2021**, *54*, 10331–10339.
- (43) Zheng, Y.; Matsuda, T.; Nakajima, T.; Cui, W.; Zhang, Y.; Hui, C.-Y.; Kurokawa, T.; Gong, J. P. How chain dynamics affects crack initiation in double-network gels.

- Proc. Natl. Acad. Sci. U.S.A.* **2021**, 118, e2111880118.
- (44) Zhang, Y.; Fukao, K.; Matsuda, T.; Nakajima, T.; Tsunoda, K.; Kurokawa, T.; Gong, J. P. Unique crack propagation of double network hydrogels under high stretch. *Extreme Mech. Lett.* **2022**, 51, 101588.
- (45) Zhu, S.; Wang, Y.; Wang, Z.; Chen, L.; Zhu, F.; Ye, Y.; Zheng, Y.; Yu, W.; Zheng, Q. Metal-Coordinated Dynamics and Viscoelastic Properties of Double-Network Hydrogels. *Gels* **2023**, 9, 145.
- (46) Jia, Y.; Zhou, Z.; Jiang, H.; Liu, Z. Characterization of fracture toughness and damage zone of double network hydrogels. *J. Mech. Phys. Solids.* **2022**, 169, 105090.
- (47) Kolvin, I.; Kolinski, J. M.; Gong, J. P.; Fineberg, J. How supertough gels break. *Phys. Rev. Lett.* **2018**, 121, 135501.
- (48) Nakajima, T.; Kurokawa, T.; Ahmed, S.; Wu, W.-l.; Gong, J. P. Characterization of internal fracture process of double network hydrogels under uniaxial elongation. *Soft Matter* **2013**, 9, 1955–1966.
- (49) Zheng, Y.; Nakajima, T.; Cui, W.; Hui, C.-Y.; Gong, J. P. Swelling Effect on the Yielding, Elasticity, and Fracture of Double-Network Hydrogels with an Inhomogeneous First Network. *Macromolecules* **2023**, 56, 3962–3972.
- (50) Matsuda, T.; Nakajima, T.; Fukuda, Y.; Hong, W.; Sakai, T.; Kurokawa, T.; Chung, U.-i.; Gong, J. P. Yielding criteria of double network hydrogels. *Macromolecules* **2016**, 49, 1865–1872.
- (51) Wang, S.; Hu, Y.; Kouznetsova, T. B.; Sapir, L.; Chen, D.; Herzog-Arbeitman, A.; Johnson, J. A.; Rubinstein, M.; Craig, S. L. Facile mechanochemical cycloreversion of polymer cross-linkers enhances tear resistance. *Science* **2023**, 380, 1248–1252.
- (52) Zheng, D.; Lin, S.; Ni, J.; Zhao, X. Fracture and fatigue of entangled and unentangled polymer networks. *Extreme Mech. Lett.* **2022**, 51, 101608.
- (53) Kim, J.; Zhang, G.; Shi, M.; Suo, Z. Fracture, fatigue, and friction of polymers in which entanglements greatly outnumber cross-links. *Science* **2021**, 374, 212–216.
- (54) Zhou, Y.; Hu, J.; Zhao, P.; Zhang, W.; Suo, Z.; Lu, T. Flaw-sensitivity of a tough hydrogel under monotonic and cyclic loads. *J. Mech. Phys. Solids.* **2021**, 153, 104483.

- (55) Liu, C.; Mayumi, K.; Hayashi, K.; Jiang, L.; Yokoyama, H.; Ito, K. Direct Observation of Large Deformation and Fracture Behavior at the Crack Tip of Slide-Ring Gel. *J. Electrochem. Soc.* **2019**, 166, B3143–B3147.
- (56) Liu, C.; Kadono, H.; Yokoyama, H.; Mayumi, K.; Ito, K. Crack propagation resistance of slide-ring gels. *Polymer* **2019**, 181, 121782–121782.

For Table of Contents Use Only

